enhancing effect of the *ortho*-methoxy substituents is steric in nature. This is confirmed by the fact that no decrease in catalyst activity was observed when an excess of **1** was used, in contrast with the Pd/DPPPr-S/HOTs system, where the reaction is almost completely inhibited when two equivalents of ligand are added.[5b] Apparently, catalytically inactive $[\mathrm{Pd^{II}}(\mathrm{D}\text{-}o\text{-}\mathrm{APPr\text{-}S})_2]$ complexes cannot be formed with **1**.

The presence of the *ortho*-methyl groups in **6** did not induce a similar rate-enhancing effect, which suggests that the effect of the *ortho*-methoxy substituents in **1** is not only steric. The oxygen atoms might coordinate to the palladium atom at some stages during the reaction to stabilize energetically less favorable configurations.[9] Nevertheless, a permanent coordinative bond with the oxygen atom was not observed in the NMR spectra of **2**–**4**. When the monodentate $\mathrm{P(C_6H_3\text{-}2\text{-}OCH_3\text{-}5\text{-}SO_3Na)_3}$ was used as ligand, catalyst decomposition took place, showing that the copolymerization does not proceed in the presence of a P ~ O chelate alone, but requires a P ~ P ligand.

Although the alternating copolymerization of ethene and CO is initially homogeneous, in a later stage the growing polymer precipitates and the reaction might proceed heterogeneously. Indeed, when we recovered the Pd/D-*o*-APPr-S catalyst by filtering off the product, only traces of copolymer were formed in a second run. This indicates that the catalyst was still attached to the polymer chain, which is precipitated on the rest of the product. Nonetheless, by introducing a "termination procedure" (see supporting information) 61 % of the catalyst activity could be restored.[10]

The Pd/D-*o*-APPr-S catalyst was also active in a supported aqueous phase (SAP) system, in which the copolymer itself is used as a support for an aqueous catalyst solution, which is distributed as a thin film over the surface. Such a "gas-phase process" minimizes the amount of solvent needed in the process and avoids fouling of the reaction vessel. In this SAP system, under nonoptimized conditions (90 °C, 60 bar), catalyst activities of 21.3 $\mathrm{kg\,g\,Pd^{-1}\,h^{-1}}$ were reached.

In conclusion, we have developed a simple, highly active, air-stable, and environmentally friendly catalyst for the alternating copolymerization of ethene and CO.

Received: September 2, 1999 [Z 13953]

---

[1] a) A. Sen, *Acc. Chem. Res.* **1993**, *26*, 303; b) E. Drent, P. H. M. Budzelaar, *Chem. Rev.* **1996**, *96*, 663; c) A. Sommazzi, F. Garbassi, *Prog. Polym. Sci.* **1997**, *22*, 1547.

[2] a) E. Drent (Shell), EP-B 121965, **1984** [*Chem. Abstr.* **1985**, *102*, 46423t]; b) E. Drent, J. A. M. van Broekhoven, M. J. Doyle, *J. Organomet. Chem.* **1991**, *417*, 235.

[3] E. Drent, R. L. Wife (Shell), EP-B 222454, **1987** [*Chem. Abstr.* **1987**, *107*, 199098u].

[4] a) F. Joó, A. Kathó, *J. Mol. Catal. A* **1997**, *116*, 3; b) G. Papadogianakis, R. A. Sheldon in *Catalysis*, *Vol. 13* (Ed.: J. J. Spivey), Royal Society of Chemistry, London, **1997**, pp. 114–193; c) *Aqueous-Phase Organometallic Catalysis* (Eds.: B. Cornils, W. A. Herrmann), WILEY-VCH, Weinheim, **1998**; d) G. Verspui, G. J. ten Brink, R. A. Sheldon, *Chemtracts: Org. Chem.* **1999**, *12*, 777.

[5] a) Z. Jiang, A. Sen, *Macromolecules* **1994**, *27*, 7215; b) G. Verspui, G. Papadogianakis, R. A. Sheldon, *Chem. Commun.* **1998**, 401; c) C. Bianchini, H. M. Lee, A. Meli, S. Monetti, V. Patinec, G. Petrucci, F. Vizza, *Macromolecules* **1999**, *32*, 3859.

[6] G. Verspui, F. Schanssema, R. A. Sheldon, *Appl. Catal. A* **1999**, in press.

[7] a) G. P. C. M. Dekker, C. J. Elsevier, K. Vrieze, P. W. N. M. van Leeuwen, *Organometallics* **1992**, *11*, 1598; b) G. P. C. M. Dekker, C. J. Elsevier, K. Vrieze, P. W. N. M. van Leeuwen, C. F. Roobeek, *J. Organomet. Chem.* **1992**, *430*, 357.

[8] Recently, we observed by NMR spectroscopy the formation of $[\mathrm{Pd(H)\{P(C_6H_4\text{-}\mathit{m}\text{-}SO_3Na)_3\}_3}]^+$ by reduction of a $\mathrm{Pd^{II}}$ complex with CO in a strongly acidic aqueous medium: G. Verspui, I. I. Moiseev, R. A. Sheldon, *J. Organomet. Chem.* **1999**, *586*, 196.

[9] The coordination of *ortho*-$\mathrm{OCH_3}$ substituents was observed in the solid state in $[\mathrm{Pd\{P(C_6H_2\text{-}2,4,6\text{-}(OMe)_3)_3\}_2}](\mathrm{BF_4}^-)_2$; K. R. Dunbar, J.-S. Sun, *J. Chem. Soc. Chem. Commun.* **1994**, 2387.

[10] Termination can occur by hydrolysis of a Pd–acyl bond or by a rearrangement of a Pd–alkyl intermediate analogous to **4** to an enolate complex followed by a subsequent hydrolysis reaction; M. A. Zuideveld, P. C. J. Kamer, P. W. M. N. van Leeuwen, P. A. A. Klusener, H. A. Stil, C. F. Roobeek, *J. Am. Chem. Soc.* **1998**, *120*, 7977.

Generation-Dependent Intramolecular CT Complexation in a Dendrimer Electron Sponge Consisting of a Viologen Skeleton

Susanne Heinen and Lorenz Walder*

In the last two decades efficient methodologies for the cascade synthesis of dendrimers have been developed. Nowadays the main research activities are focused on dendritic effects resulting from the topology and the interaction of built-in molecular functionalities.[1] Redox-active subunits play an important role in this respect. They may be located: a) in the core,[2, 3] b) in the periphery,[4–7] or c) in the core, the branches, and the periphery of the dendrimer.[8–11] The resulting dendritic effects concern redox protein mimetics,[3] redox gradients,[11] charge transfer (CT) complex-based conductivity,[7] electron sponges,[4] and redox sensors.[12]

We present here a new homologous series of electroactive dendrimers belonging to class (c). The dendrimers consist of a viologen skeleton that contains up to 45 electrochemically accessible 4,4′-bipyridinium subunits which cause electron sponge properties. Electrochemical measurements revealed an excellent correlation between the hydrodynamic radius and the generation number of the dendrimers. Furthermore, an electrochemically switchable and generation-dependent CT complex was observed for the first time in the cation radical oxidation state.

The synthesis of the dendrimers of generations zero to three follows the "divergent method with preformed branching units" (Scheme 1).[13] The well-known trifunctional initiator core $\mathbf{P0}\cdot 3\,\mathrm{PF_6}^-$ consists of a mesityl derivative linked to three 4,4′-bipyridinium units.[14] The three peripheral nitrogens react quantitatively with primary benzyl or alkyl bromides or iodides. 1,3-Di-(hydroxymethyl)-benzyl bromide (**V1**)

---

[*] Prof. Dr. L. Walder, Dipl. Chem. S. Heinen
Institut für Chemie, OCII
Universität Osnabrück
Barbarastrasse 7, 49069 Osnabrück (Germany)
Fax: (+49) 541-969-12-58
E-mail: LoWalder@rz.uni-osnabrueck.de

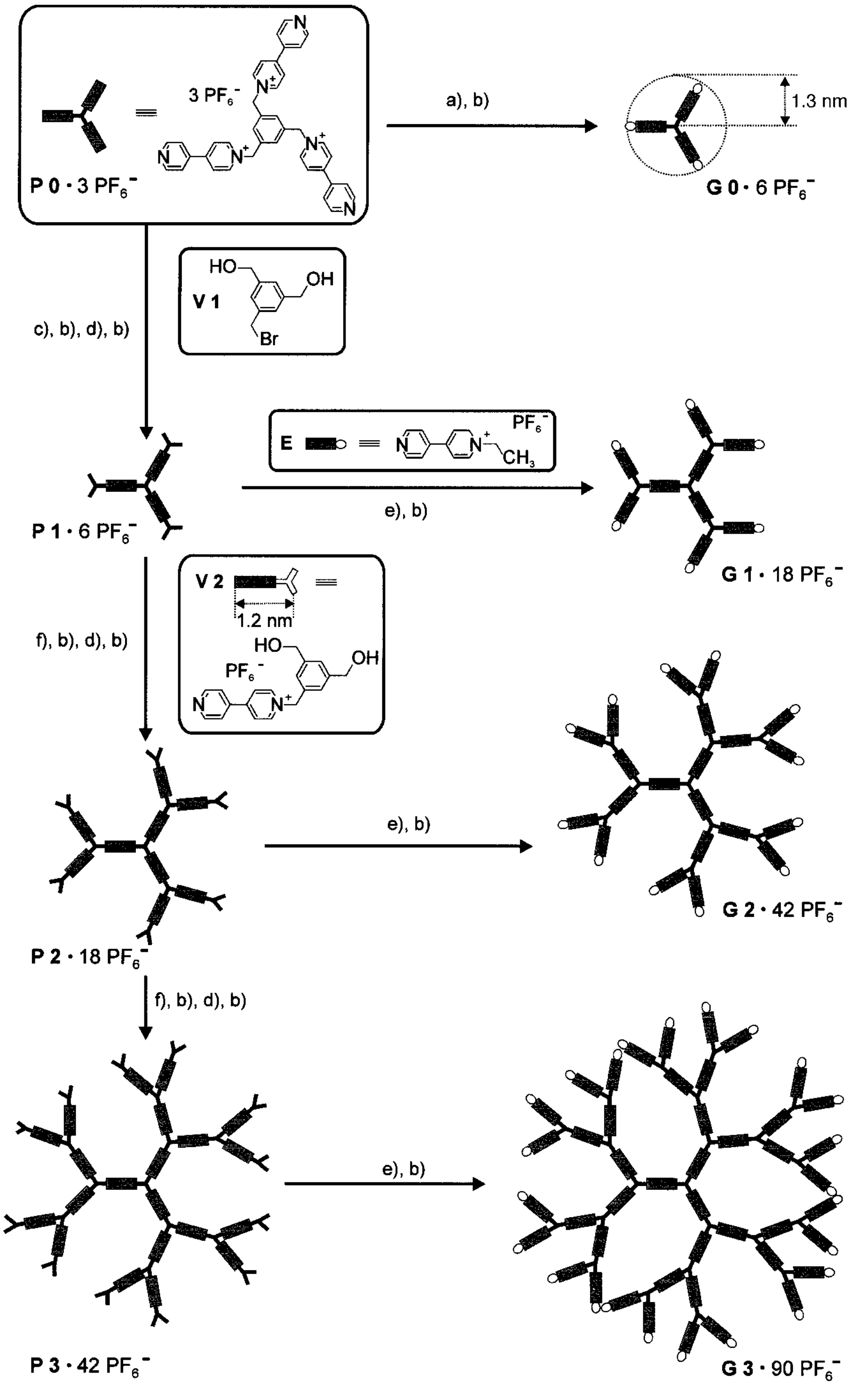

Scheme 1. Synthesis of the dendritic polycations **G0** to **G3**; a) EtI/MeCN; b) NH_4PF_6/H_2O; c) **V1**/MeCN; d) HBr/AcOH; e) **E**/MeCN; f) **V2**/MeCN.

plays the role of the "preformed branching unit". The resulting hexol was activated by conversion into the corresponding hexabromide **P1** · 6 PF_6^-. The direct reaction of **P0** · 3 PF_6^- with 1,3,5-tris(bromomethyl) benzene failed because of inter- and intramolecular crosslinking. The branching unit **V2**, equipped with a reactive pyridine nitrogen and two benzylic alcohols, was used for the preparation of the precursors **P2** · 18 PF_6^- and **P3** · 42 PF_6^-. The higher dendrimer precursors were grown from **P1** · 3 PF_6^- by repetitive application of the reaction steps (f), (b), and (d). In order to solubilize the intermediates it was necessary to exchange the counter ion after each reaction step (b). The dendrimer **G0** · 6 PF_6^- was available from its precursor via alkylation with ethyl iodide followed by ion exchange, whereas the dendrimers **G1** to **G3** where obtained from the reactions of *N*-ethyl-4,4′-bipyridinium hexafluorophosphate (**E**) with the corresponding precursors in good yields as hexafluorophosphate salts. The products were pure by NMR spectroscopy and by elemental analysis, apart from a variable water content (see Experimental Section). MALDI-TOF mass spectrometry experiments were not successful, probably because of the high charge present in these compounds.[15]

The dendrimers **G0** to **G3** exhibit two chemically reversible waves in cyclic voltammetry (DMF/0.1 M TBAPF$_6$, TBA = *t*BuN$^+$), similar to those of monomeric dibenzyl viologen, with peak separations in the range of 70–80 mV at scan rates up to 100 mV s^{-1}. The shape of the second wave indicates adsorption of the neutral compound on the electrode surface. The redox centers within the dendrimers do not exhibit strong intramolecular interactions, except for a weak coulombic destabilization of the dicationic oxidation state, resulting in a trend towards more positive E_1^0 values with increasing generations (n) (Table 1). The number of exchanged electrons per molecule (n_{exp}), as measured by preparative electrolysis coulometry, agrees with the calculated value (n_{theor}) to within 95 % (Table 1). The diffusion limited currents (i_l) for the reduction of dendrimers **G0** to **G3** were obtained with a rotating disk electrode; they fulfil the Levich equation ($i_l \sim \omega^{1/2}$, ω = angular velocity) and were used to calculate the diffusion coefficient D_{exp} (Table 1 and Figure 1 a).[16] From the diffusion coefficients the hydrodynamic radii r_h (Table 1) were calculated with the Stokes equation, with the assumption of hard spheres. However, according to MM$^+$ calculations[17] even **G3** is ellipsoidal rather than spherical (r_{1calcd} and r_{2calcd}, Table 1). The experimental radii (r_h) lie between the large and small calculated radii of the ellipsoid. In Figure 1 b the experimental radii are plotted against the generation number. A linear dependence with a slope of 0.86 nm generation^{-1}, a *y*-intercept of 1.16 nm, and an excellent correlation factor R^2 of 0.9968 is observed. The value from the slope corresponds to 72 % of the theoretical length of the mesityl bipyridinium inserted per generation (ca. 1.2 nm).[17]

A novel, dendrimer generation-dependent and electrochemically switchable CT complexation was observed. All dendrimers show reversible behavior under spectroelectro-

Table 1. Physical Chemical Data and Simulation Results

	G0	G1	G2	G3
M [g mol^{-1}]	1542.7	4658.1	10888.9	23350.4
E_1^0 [mV][a]	-310	-295	-275	-252
n_{exp}[b]	2.9	9.1	20.4	43.4
n_{theor}[b]	3	9	21	45
D_{exp} [cm^{2}s^{-1}][c]	2.05×10^{-6}	1.23×10^{-6}	8.8×10^{-7}	6.5×10^{-7}
r_h [nm][d]	1.2 ± 0.1	2 ± 0.2	2.8 ± 0.2	3.8 ± 0.2
$r_{1\,calcd}$, $r_{2\,calcd}$ [nm][e]	1.3, 0.4	2.6, 1.8	3.7, 2.6	4.6, 3.7
P_{tot} [%][f]	7.4	23.6	25.1	29.3
P_{per} [%][g]	(11.2)	36	44	55

[a] First reduction potential determined by spectroelectrochemistry (DMF/0.1M TBAPF$_6$, against Ag/AgCl). [b] Number of electrons transferred per molecule theoretically (n_{theor}) and as determined by electrolysis (n_{exp}). [c] Diffusion coefficient from the diffusion limited current with the rotating disk electrode according to the Levich equation.[16] [d] Hydrodynamic radius from D_{exp} according to the Stokes equation. [e] Large and small radii of the ellipsoid from MM$^+$ simulations.[17] [f] Degree of pimerization (from analysis of the visible spectra at 537 and 605 nm) with respect to all viologen centers. [g] Degree of pimerization (from analysis of the visible spectra at 537 and 605 nm) with respect to the viologen centers in the outermost dendrimer shell.

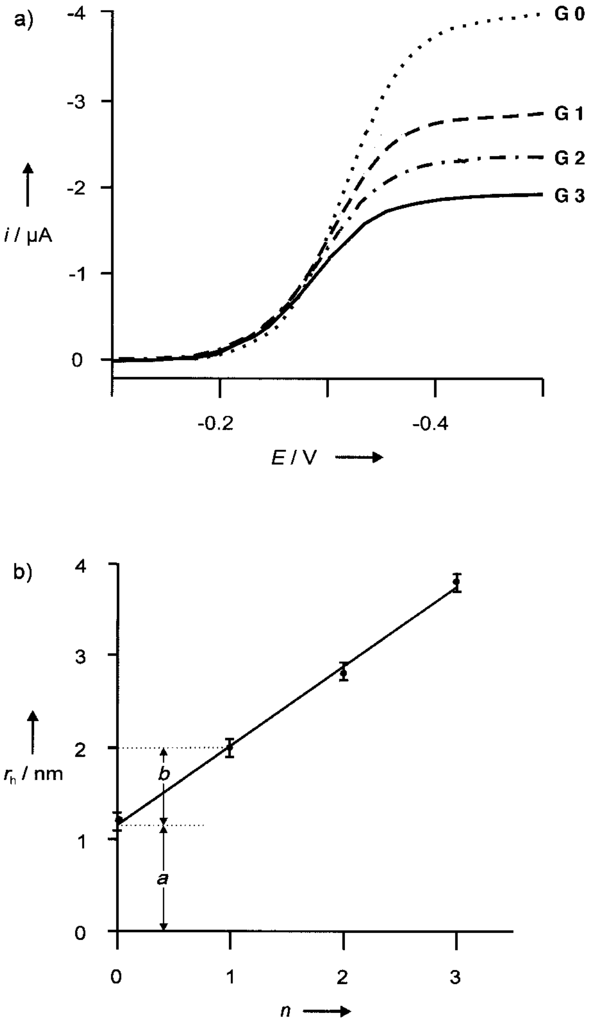

Figure 1. a) Current–potential curves for the reduction of **G0** to **G3** with the rotating disk electrode at constant viologen subunit concentration ($n_{theor}\,c$(dendrimer)). From the plateau currents the diffusion coefficients were calculated. b) Hydrodynamic radii r_h [nm] as a function of the generation number n; y-intercept $a = 1.16$ nm, slope $b = 0.86$ nm generation^{-1}.

chemical conditions (preparative electrolysis in combination with a flow-through cuvette); they show complete decoloration at 0 V and blue to violet coloration if reduced at -0.48 V against Ag/AgCl. The absorption bands at 370, 540, and 800–1100 nm in the visible spectrum indicate the presence of "pimers", CT complexes between two radical cations.[18] The degree of pimerization in the reduced **G0** to **G3** was evaluated by quantitative comparison of the cation radical dimer spectra with data from literature for pure pimers and pure monomeric radical cations (Table 1, Figure 2).[18] Surprisingly, the degree of pimerization (P_{tot}) grows with rising generation numbers (Figure 2). From the literature it is known that pimerization is strongly distance dependent. As the relative intensity of the CT adsorption bands showed no influence on the concentration of the dimers, pimerization must be related to intramolecular interactions of cation radicals. We believe that the probability for a cisoid conformation of two *meta*-positioned viologen radical cations in the outermost dendrimer shell—a prerequisite for pimer formation—becomes increasingly larger for higher generation numbers. In accordance with this model, an approximately linear increase of the degree of pimerization related to the outermost shell (P_{per}) with the generation number is observed (Figure 2b).

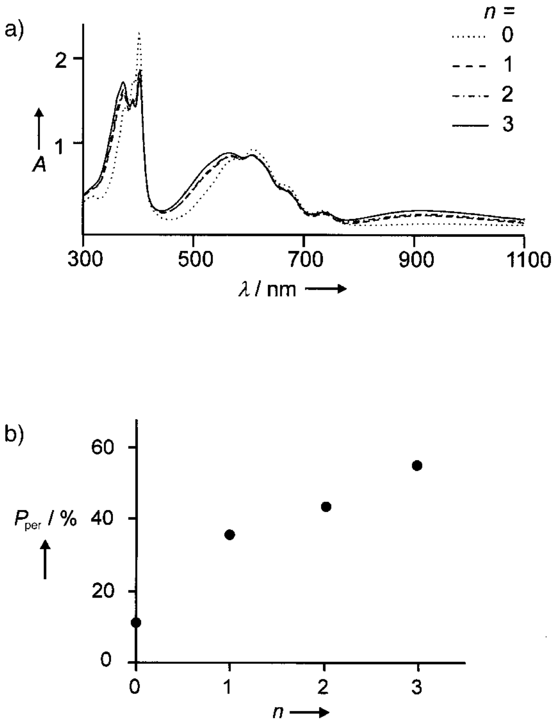

Figure 2. a) Generation-dependent pimerization: UV–Visible spectra of the 3-, 9-, 21- and 45-electron reduced **G0**, **G1**, **G2**, and **G3** at $n_{theor}\,c$(dendrimer) $= 3.8 \times 10^{-4}$ M (Spectroelectrochemical cell with a length of 2 mm). b) Degree of pimerization in the outermost peripheral shell from analysis of the adsorption at 537 and 605 nm as a function of the generation number n.

We are currently exploring the possibilities for using these observed CT properties in combination with association reactions for molecular recognition/signal transduction.

0570-0833/00/3904-0808 $ 17.50+.50/0

Experimental Section

Conditions for ^{1}H NMR data: 250 MHz, CD_3CN, 25 °C, TMS; for ^{13}C NMR data: 63 MHz, CD_3CN, 25 °C, TMS.

G0 $\cdot 6PF_6^-$: ^{1}H NMR: $\delta = 8.92$ (d, ^3J(H,H) = 7.0 Hz, 12 H), 8.39 (d, ^3J(H,H) = 7.0 Hz, 12 H), 7.66(s, 3 H), 5.83 (s, 6 H), 4.68 (q, ^3J(H,H) = 7.3 Hz, 6 H), 1.65 (t, ^3J(H,H) = 7.3 Hz, 9 H); ^{13}C NMR: $\delta = 151.1$, 150.1, 146.2, 145.8, 135.3, 132.3, 127.8, 127.6, 64.0, 58.2, 16.0; elemental analysis calcd for $C_{45}H_{48}N_6P_6F_{36} \cdot 1H_2O$: C 34.63, H 3.23, N 5.39; found C 34.85, H 3.58, N 5.36.

G1 $\cdot 18PF_6^-$: ^{1}H NMR: $\delta = 8.93-8.90$ (m, 36 H), 8.42–8.36 (m, 36 H), 7.66(s, 9 H), 7.64(s, 3 H), 5.83 (s, 24 H), 4.67(q, ^3J(H,H) = 7.3 Hz, 12 H), 1.65 (t, ^3J(H,H) = 7.3 Hz, 18 H); ^{13}C NMR: $\delta = 151.1$, 151.0, 150.1, 146.3, 146.2, 145.8, 135.3, 132.3, 132.2, 127.9, 127.8, 127.6, 64.0, 58.2, 16.0; elemental analysis calcd for $C_{138}H_{138}N_{18}P_{18}F_{108} \cdot 3H_2O$: C 35.18, H 3.08, N 5.35; found C 35.13, H 3.21, N 5.32.

G2 $\cdot 42PF_6^-$: ^{1}H NMR: $\delta = 8.93-8.90$ (m, 84 H), 8.41–8.39 (m, 84 H), 7.66 (br. s, 30 H), 5.83 (s, 60 H), 4.67(q, ^3J(H,H) = 7.3 Hz, 24 H), 1.64 (t, ^3J(H,H) = 7.2 Hz, 36 H); ^{13}C NMR: $\delta = 151.1$, 151.0, 150.1, 146.2, 145.7, 135.3, 135.2, 132.2, 132.1, 127.9, 127.8, 127.6, 64.0, 58.1, 15.9; elemental analysis calcd for $C_{324}H_{318}N_{42}P_{42}F_{252}{}^* \cdot 5H_2O$: C 35.45, H 3.01, N 5.36; found C 35.23, H 3.01, N 5.33.

G3 $\cdot 90PF_6^-$: ^{1}H NMR: $\delta = 8.93-8.90$ (m, 180 H), 8.42–8.39 (m, 180 H), 7.67 (br. s, 66 H), 5.83 (s, 132 H), 4.67(q, ^3J(H,H) = 7.3 Hz, 48 H), 1.64 (t, ^3J(H,H) = 7.2 Hz, 72 H); ^{13}C NMR: $\delta = 151.1$, 151.0, 146.2, 145.7, 135.3, 135.2, 132.2, 127.9, 127.8, 127.6, 64.0, 58.1, 15.9; elemental analysis calcd for $C_{696}H_{678}N_{90}P_{90}F_{540} \cdot 23H_2O$: C 35.18, H 3.07, N 5.30; found C 35.02, H 3.18, N 5.23.

Received: August 18, 1999 [Z 13896]

---

[1] A. Archut, F. Vögtle, *Chem. Soc. Rev.* **1998**, *27*, 233–240.
[2] H. F. Chow, I. Y. K. Chan, C. C. Mak, *Tetrahedron Lett.* **1995**, *36*, 8633–8636.
[3] P. J. Dandliker, F. Diederich, A. Zingg, J. P. Gisselbrecht, M. Gross, A. Louati, E. Sanford, *Helv. Chim. Acta* **1997**, *80*, 1773–1801.
[4] F. Moulines, L. Djakovitch, R. Boese, B. Gloaguen, W. Thiel, J. L. Fillaut, M. H. Delville, D. Astruc, *Angew. Chem.* **1993**, *105*, 1132–1134; *Angew. Chem. Int. Ed. Engl.* **1993**, *32*, 1075–1077.
[5] C. F. Shu, H. M. Shen, *J. Mater. Chem.* **1997**, *7*, 47–52.
[6] G. D. Storrier, K. Takada, H. D. Abruna, *Langmuir* **1999**, *15*, 872–884.
[7] L. L. Miller, R. G. Duan, D. C. Tully, D. A. Tomalia, *J. Am. Chem. Soc.* **1997**, *119*, 1005–1010.
[8] G. R. Newkome, R. Guther, C. N. Moorefield, F. Cardullo, L. Echegoyen, E. Perezcordero, H. Luftmann, *Angew. Chem.* **1995**, *107*, 2159–2162; *Angew. Chem. Int. Ed. Engl.* **1995**, *34*, 2023–2026.
[9] V. Balzani, S. Campagna, G. Denti, A. Juris, S. Serroni, M. Venturi, *Acc. Chem. Res.* **1998**, *31*, 26–34.
[10] M. Osawa, M. Hoshino, S. Horiuchi, Y. Wakatsuki, *Organometallics* **1999**, *18*, 112–114.
[11] T. D. Selby, S. C. Blackstock, *J. Am. Chem. Soc.* **1998**, *120*, 12155–12156.
[12] C. Valerio, J. L. Fillaut, J. Ruiz, J. Guittard, J. C. Blais, D. Astruc, *J. Am. Chem. Soc.* **1997**, *119*, 2588–2589.
[13] N. Ardoin, D. Astruc, *Bull. Soc. Chim. Fr.* **1995**, *132*, 875–909.
[14] D. B. Amabilino, P. R. Ashton, M. Belohradsky, F. M. Raymo, J. F. Stoddart, *Chem. Commun.* **1995**, 751–753.
[15] P. R. Ashton, K. Shibata, A. N. Shipway, J. F. Stoddart, *Angew. Chem.* **1997**, *109*, 2902–2905; *Angew. Chem. Int. Ed.* **1997**, *36*, 2781–2783.
[16] D. T. Sawyer, J. L. Roberts, Jr., *Experimental Electrochemistry for Chemists*, 1st ed., Wiley, NY, **1974**, p. 93.
[17] Structures were modeled and optimized in the gas phase and without consideration of the counter ions using the MM$^+$-program Hyperchem 5.0; Hyperchem, Hypercube, Inc., 1115 NW 4th Street, Gainesville, FL 32601 (USA).
[18] W. Geuder, S. Hünig, A. Suchy, *Tetrahedron* **1986**, 1665–1677.

A Redox-Controlled Molecular Switch Based on the Reversible C–C Bond Formation in Octamethoxytetraphenylene**

Rajendra Rathore,* Pierre Le Magueres,
Sergey V. Lindeman, and Jay K. Kochi*

The design and synthesis of organic derivatives for molecular devices such as sensors, switches, electrical conductors, ferromagnets, electronic circuits, and nonlinear optical materials has been actively pursued in recent years. [1–3] Especially noteworthy are organic materials that exhibit changes in physical properties such as magnetism, conductivity, and optical response when triggered by external stimuli such as heat, light, or electrical potentials.[4] One of the approaches in designing such materials is to exploit electronic interactions in macrocyclic or supramolecular assemblies consisting of multiple redox-active components.[5] We now introduce a methoxylated tetraphenylene derivative as a potential molecular switch based on its dramatic color change upon the application of an electrical potential.

Octamethoxytetraphenylene[6] (OMT) was prepared from a readily available 1,2-dimethoxybenzene derivative (veratrole) in excellent yield using standard synthetic procedures (see Experimental Section). This saddle-shaped macrocycle with cofacial phenylene groups (established by X-ray crystallography) shows a striking electrochromic behavior with a color change from yellow to red, which is completely reversible over multiple redox cycles [Eq. (1)].[7]

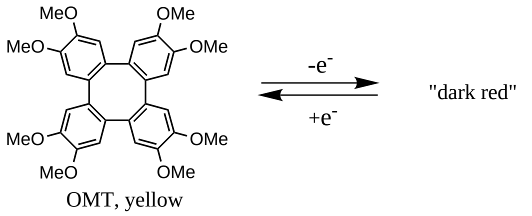

(1)

The dramatic color change upon electrooxidation of OMT can also be achieved by a variety of chemical oxidants such as aromatic radical cations,[8] nitrosonium cation,[9] or triethyloxonium hexachloroantimonate.[10] For example, a blue solution of a octahydronaphthacene radical cation[11] ($NAP^{\bullet+}$) turns dark red immediately upon the addition of neutral OMT [Eq. (2)]. In order to establish the stoichiometry of this

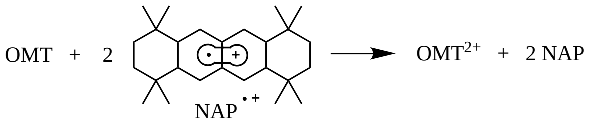

(2)

---

[*] R. Rathore, J. K. Kochi, P. Le Magueres, S. V. Lindeman
Department of Chemistry, University of Houston
Houston, TX 77204-5641 (USA)
Fax: (1) 713-743-2709
E-mail: rrathore@bayou.uh.edu, jkochi@pop.uh.edu

[**] We thank J. Hecht for the preliminary experiments and the National Science Foundation and Robert A. Welch Foundation for financial support.